

Efficient correction of multiqubit measurement errors

Michael R. Geller¹ and Mingyu Sun^{1,*}

¹*Center for Simulational Physics, University of Georgia, Athens, Georgia 30602, USA*

(Dated: May 5, 2022)

State preparation and measurement (SPAM) errors limit the performance of noisy intermediate-scale quantum computers and their potential for practical application. SPAM errors are partly correctable after a calibration step that requires, for an exact implementation on a register of n qubits, 2^n additional characterization experiments. Here we introduce an approximate but efficient method for multiqubit SPAM error characterization and correction requiring the classical processing of $2^n \times 2^n$ matrices, but only $O(2^k n^2)$ measurements, where $k = O(1)$ is the number of qubits in a correlation volume. We demonstrate and validate the technique using IBM Q online quantum computers on registers of up to 9 superconducting qubits.

I. INTRODUCTION

Errors in a quantum computation are typically classified into state-preparation errors, gate errors, and read-out or measurement errors. Quantum error correction has mostly focused on gate errors, in part because state preparation and measurement (SPAM) errors only occur at the beginning and end of a circuit or error-correction cycle, and, unlike gate errors, do not accumulate with circuit depth [1]. One consequence of this is that surface code error correction, a practical route to fault-tolerant quantum computation, is significantly less sensitive to measurement errors than to gate errors, tolerating errors many times larger [2].

However in noisy intermediate-scale quantum (NISQ) devices, which are not error corrected, SPAM errors are large and, even worse, may increase with register size due to increased crosstalk. A standard approach for correcting some of the SPAM error is to measure the overlap-squared matrix between all initial and final classical states, and use this information to classically correct the measured data [3–11]. We refer to this technique as T matrix error correction or error mitigation.

II. T MATRIX ERROR CORRECTION

The technique can be described as follows: Let $x, x' \in \{0, 1\}^n$ be classical states of n qubits, and define the elements of a $2^n \times 2^n$ transition matrix T by

$$T(x|x') = T(x_1 \cdots x_n | x'_1 \cdots x'_n) = \text{Tr}[E_{x_1 \cdots x_n} \rho_{x'_1 \cdots x'_n}]. \quad (1)$$

Here E_x is the multiqubit POVM effect characterizing the nonideal implementation of the projector $|x\rangle\langle x|$, and $\rho_{x'}$ is the density matrix produced after attempting to prepare classical state $|x'\rangle\langle x'|$. Each column of T is the

raw probability distribution $\text{prob}(x)$ measured immediately after preparing x' . Let the set of n physical qubits used to measure T be called the *register*. The register does not have to include every qubit in the device.

Ideally $T(x|x') = \delta_{xx'}$, the $2^n \times 2^n$ identity. The exact implementation of the error correction technique is to measure T and classically apply T^{-1} to subsequently measured probability distributions [3–11]. This forces an empty circuit in the noisy register to behave ideally.

However there are several problems with T matrix SPAM correction: (1) An exact implementation requires 2^n characterization experiments (probability measurements), which is not scalable. The classical processing of the calibration data is also inefficient. (2) The matrix T may become singular for large n , preventing direct inversion. (3) The inverse T^{-1} might not be a stochastic matrix, meaning that it can produce negative corrected probabilities [12]. (4) The correction is not rigorously justified, so we cannot be sure that we are only removing SPAM errors and not otherwise corrupting an estimated probability distribution.

Limitations (1) and (2) can be circumvented [7, 9, 10] by approximating T with a tensor product of single-qubit transition matrices T_i ,

$$T_{\text{prod}} = T_1 \otimes T_2 \otimes \cdots \otimes T_n, \quad (2)$$

$$T_{\text{prod}}^{-1} = T_1^{-1} \otimes T_2^{-1} \otimes \cdots \otimes T_n^{-1}. \quad (3)$$

Each T_i is a 2×2 matrix with elements $T_i(x_i|x'_i)$, measured by initializing qubit i with classical state $x'_i \in \{0, 1\}$ and measuring the reduced probability distribution

$$\text{prob}(x_i) = \left(\prod_{j \neq i} \sum_{x_j=0}^1 \right) \text{prob}(x_1 x_2 \cdots x_n). \quad (4)$$

In this work we go beyond the product approximation (2) by deriving an efficient yet accurate method to estimate T . The technique is efficient in the sense that it only requires $O(n^2)$ probability measurements to estimate the entire set of 4^n matrix elements $\{T(x|x')\}_{x,x'}$. However evaluating these 4^n matrix elements from the measured

* mingyu.sun25@uga.edu

data remains classically inefficient. While transition-matrix SPAM correction might ultimately be unscalable, we hope that the technique introduced in this paper will enable error mitigation on large registers of qubits, greatly extending the reach and power of NISQ computing. Beyond its use to correct SPAM errors, the estimated T matrix can also be used to rapidly characterize and quantify correlated SPAM errors, including measurement crosstalk. We demonstrate this here on three different IBM Q online devices, allowing us to compare multiqubit SPAM errors across different chips.

The exact T matrix SPAM correction technique based on (1) is not scalable because it does not make use of (i) the tensor product structure of the physical system and the fact that qubits are composed of systems or devices that mainly interact pairwise, and (ii) the expectation that for large enough devices multiqubit correlations will be finite-ranged and should decay (at least algebraically) at large distances.

III. SCALABLE T MATRIX ESTIMATION

Here we explain in detail the technique of scalable T matrix estimation.

A. Uncovering the tensor product structure

The tensor product structure and locality are the keys to scalability. However these properties are not immediately apparent in the definition (1), and are not rigorously present without an additional continuity assumption: To each physical system or device we introduce an associated *noninteracting* qubit array consisting of a register of n qubits, each (optionally) coupled to its own independent measurement apparatus, but with no cross coupling between qubits or detectors [13]. Our assumption is that states of the interacting and noninteracting systems are related by a completely positive trace-preserving (CPTP) map,

$$\rho_{x'} = \Lambda(\rho_{x'_1}^0 \otimes \cdots \otimes \rho_{x'_n}^0). \quad (5)$$

Here Λ is a CPTP superoperator. In (5) we further assume that the initial state $\rho_{x'}^0$ of the noninteracting array is separable and can be written as a product $\rho_{x'_1}^0 \otimes \cdots \otimes \rho_{x'_n}^0$ of single-qubit density matrices. A sufficient condition for (5) to hold is that the ground and excited states of the coupled qubits can be obtained by adiabatically turning on the qubit-qubit interaction V . In this case

$$\rho_{x'} = S(\rho_{x'_1}^0 \otimes \cdots \otimes \rho_{x'_n}^0)S^\dagger, \quad (6)$$

where $S = Te^{-i\int V dt}$. However we don't require the map between the interacting and noninteracting limits to be adiabatic or even unitary. But we exclude cases where the initial state of the uncoupled register is entangled with

the environment, and cases where turning on the qubit-qubit coupling causes leakage out of the register; in these cases the map would not be CPTP. The transition matrix in the noninteracting array is

$$\text{Tr}[E_{x_1}^{(1)} \otimes \cdots \otimes E_{x_n}^{(n)} (\rho_{x'_1}^0 \otimes \cdots \otimes \rho_{x'_n}^0)]. \quad (7)$$

Here $E_0^{(i)}$ and $E_1^{(i)} = I - E_0^{(i)}$ are two-outcome POVM elements for qubit i , which may vary from qubit to qubit. Due to detector nonidealities, the $E_{x_i}^{(i)}$ may differ from projectors, but the multiqubit measurement operators are tensor products of the single-qubit ones as the qubits are uncoupled. Then using (5) we can write (1) as

$$T(x|x') = \langle E_{x_1}^{(1)} \otimes \cdots \otimes E_{x_n}^{(n)} \rangle_{x'}, \quad (8)$$

where

$$\langle O \rangle_{x'} \equiv \text{Tr}[O\Lambda(\rho_{x'_1}^0 \otimes \cdots \otimes \rho_{x'_n}^0)] \quad (9)$$

is the expectation value after preparing the noisy classical state $x' = x'_1 x'_2 \cdots x'_n$.

To achieve T matrix estimation that is both scalable and highly accurate, we combine two steps, which are explained in Secs. III B and III C.

B. Mean and quadratic fluctuations

The first step is to define *mean fields*

$$\langle E_{x_i}^{(i)} \rangle_{x'} = \text{Tr}[E_{x_i}^{(i)} \Lambda(\rho_{x'}^0)], \quad (10)$$

for the measurement operators, and expand (8) in powers of fluctuations

$$\delta E_{x_i}^{(i)} = E_{x_i}^{(i)} - \langle E_{x_i}^{(i)} \rangle_{x'} \quad (11)$$

about these mean fields. The zeroth-order term leads to the *uncorrelated* approximation

$$T_{\text{prod}}(x|x') := T_1(x_1|x'_1) T_2(x_2|x'_2) \cdots T_n(x_n|x'_n) \quad (12)$$

for $T(x|x')$, which results in (2). Here

$$T_i(x_i|x'_i) = \langle E_{x_i}^{(i)} \rangle_{x'} \quad \text{with } x_i, x'_i \in \{0, 1\} \quad (13)$$

are the elements of a 2×2 *single-qubit* transition matrix for qubit i .

The single-qubit T matrix (13) obviously depends on the initial classical state $x'_i \in \{0, 1\}$ of qubit i . However it also depends, in principle, on the *entire* initial state $x' \in \{0, 1\}^n$ of the n -qubit register, a dependence that is evident in the definition (13) but suppressed by the $T_i(x_i|x'_i)$ notation. For example, it is tempting to assume that the single-qubit T matrix on qubit 1 does not depend the state of the other *spectator* qubits $i \neq 1$, but this assumption is incorrect in the presence of crosstalk, and ignoring it leads to large errors. The preferred way to treat spectator qubits is discussed in Sec. III C.

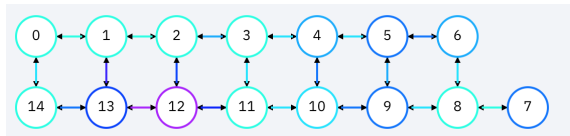


FIG. 1. Layout of IBM Q device ibmq_16_melbourne. In this work we use the n -qubit registers $Q_0, Q_1, Q_2, \dots, Q_{n-1}$ up to $n=9$.

To quantify the multiqubit correlations present in T , we define a matrix

$$T_{\text{corr}} = T - T_{\text{prod}}. \quad (14)$$

Then we calculate the leading-order corrections to T_{prod} , which are

$$T_{\text{corr}} = T_{\text{pair}} + T_{\text{triple}} + \dots \quad (15)$$

with matrix elements

$$T_{\text{pair}}(x|x') = \sum_{i < j} C_{ij}(x_i x_j | x'_i x'_j) \prod_{\ell \neq i, j} T_{\ell}(x_{\ell} | x'_{\ell}) \quad (16)$$

and

$$T_{\text{triple}}(x|x') = \sum_{i < j < k} D_{ijk}(x_i x_j x_k | x'_i x'_j x'_k) \prod_{\ell \neq i, j, k} T_{\ell}(x_{\ell} | x'_{\ell}). \quad (17)$$

Here

$$C_{ij}(x_i x_j | x'_i x'_j) = \langle \delta E_{x_i}^{(i)} \delta E_{x_j}^{(j)} \rangle_{x'} \quad (18)$$

and

$$D_{ijk}(x_i x_j x_k | x'_i x'_j x'_k) = \langle \delta E_{x_i}^{(i)} \delta E_{x_j}^{(j)} \delta E_{x_k}^{(k)} \rangle_{x'} \quad (19)$$

are measurement operator correlation functions. T_{pair} includes a sum of pair-correlators C_{ij} for each of the $n(n-1)/2$ distinct pairs of qubits. T_{triple} includes three-qubit correlators D_{ijk} for the $n(n-1)(n-2)/6$ triples.

The single-qubit transition matrices T_{ℓ} for the spectator qubits ℓ in (16) and (17) are defined in (13). As we have discussed, T_{ℓ} depends, in principle, on the entire initial state $x' \in \{0, 1\}^n$ of the n -qubit register. The same holds for C_{ij} and D_{ijk} , as is evident from their definitions (18) and (19), but suppressed by our notation.

The matrix T is a (left) stochastic matrix, consisting of columns of nonnegative real numbers (probabilities) that sum to one. This is easily seen from the definition (1):

$$\sum_x T(x|x') = \left\langle \sum_x E_x \right\rangle_{x'} = 1. \quad (20)$$

T_i and T_{prod} also have this property. It follows that T_{corr} defined in (14) satisfies $\sum_x T_{\text{corr}}(x|x') = 0$ for every x' . It is also easily seen that T_{pair} and T_{triple} satisfy

$$\forall x' : \sum_x T_{\text{pair}}(x|x') = 0 \quad (21)$$

and

$$\forall x' : \sum_x T_{\text{triple}}(x|x') = 0. \quad (22)$$

The neglected higher order terms in the series (15) also have this property, which guarantees that probability is always conserved as higher-order fluctuations are included in the model.

In the data presented here, triple correlators were significantly smaller than the pair correlators. This is apparent in Table I, which compares their magnitudes on several IBM Q online devices. Therefore in this paper we will keep only the leading-order contribution in (15) and neglect T_{triple} .

TABLE I. Magnitude of two-qubit (18) and three-qubit (19) correlators measured on different devices, maximized over qubits, initial states x' , and final states x . The layout of the melbourne chip is shown in Fig. 1. Here n is the register size.

IBM Chip	Register	n	$\max C_{ij} $	$\max D_{ijk} $
ibmqx2	$Q_0 Q_1 Q_2 Q_3 Q_4$	5	9.8e-3	4.3e-3
ibmqx4	$Q_0 Q_1 Q_2 Q_3 Q_4$	5	4.9e-2	2.1e-3
melbourne	$Q_0 Q_1 Q_2 Q_3 Q_4$	5	1.1e-2	3.9e-3
melbourne	$Q_0 Q_1 Q_2 Q_3 Q_4 Q_5 Q_6$	7	1.1e-2	3.5e-3

C. Correlation volumes

The second step of our protocol is to *filter* the set of initial classical states $x' \in \{0, 1\}^n$ that have to be prepared, reducing the total number of measurements required from 2^n to $2^k n(n-1)/2$, where $k = O(1)$ is the number of qubits in a correlation volume, which depends on the device geometry, the noise range and strength, and the desired accuracy of the estimated T .

To be precise, there are two correlation lengths or areas, both of which we generically call “volumes”. Each volume characterizes the range of two additional correlators

$$A_{ij}(x') = \langle E_0^{(i)} \rangle_{x'} - \langle E_0^{(i)} \rangle_{\text{NOT}_j(x')} \quad (23)$$

$$B_{ijl}(x') = \langle E_0^{(i)} E_0^{(j)} \rangle_{x'} - \langle E_0^{(i)} E_0^{(j)} \rangle_{\text{NOT}_l(x')} \quad (24)$$

that quantify the sensitivity of the mean and covariance of the POVM elements to the initial states of the spectator qubits. $A_{ij}(x')$ is the change in mean value $\langle E_0^{(i)} \rangle_{x'}$ when the initial state x'_j of spectator qubit $j \neq i$ is flipped. $B_{ijl}(x')$ is the change in covariance $\langle E_0^{(i)} E_0^{(j)} \rangle_{x'}$ when the initial state x'_l of spectator qubit $l \neq i, j$ is flipped.

We use (23) and (24) to separate spectator qubits into correlated and uncorrelated regions: For each qubit i in the register, and error tolerance $\epsilon_A \geq 0$, let

$$A_i = \{j : |A_{ij}(x')| > \epsilon_A, x' \in \{0, 1\}^n\} \quad (25)$$

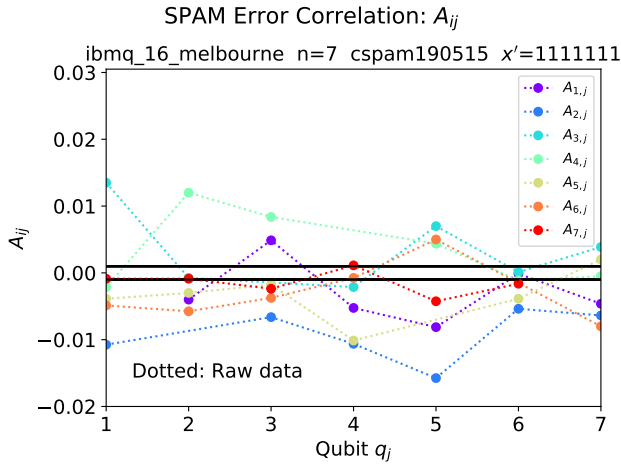


FIG. 2. A_{ij} correlator, defined in (23), used to obtain the correlation neighborhoods \mathcal{A}_i . The horizontal lines indicate the tolerance $\epsilon_A = 10^{-3}$.

be the set of qubits $j \neq i$ such that there is an A_{ij} correlator for some x' exceeding ϵ_A in magnitude. Our locality assumption implies that, for each i , the size $|\mathcal{A}_i|$ of \mathcal{A}_i (the number of correlated neighbors) is $O(1)$. And for each qubit pair $i < j$ in the register, and bound $\epsilon_B \geq 0$, let

$$\mathcal{B}_{ij} = \{l : |B_{ijl}(x')| > \epsilon_B, x' \in \{0, 1\}^n\} \quad (26)$$

be the set of qubits $l \neq i, j$ such that there is a B_{ijl} exceeding ϵ_B . By locality, $|\mathcal{B}_{ij}|$ is also $O(1)$. \mathcal{A}_i and \mathcal{B}_{ij} are called *correlation neighborhoods*, and we call the region (length or area) of qubits in a correlation neighborhood the correlation volume.

Knowledge of the correlation neighborhoods are required to evaluate the mean values (13) and covariances (18). For each qubit i , the single-qubit transition matrix (13) is to be measured for each initial state of the spec-

tator qubits in the correlation neighborhood \mathcal{A}_i . There are $2^{|\mathcal{A}_i|}$ such initial states to consider. Spectator qubits outside of \mathcal{A}_i can be initialized to any convenient state such as $|0\rangle$. Similarly, for each qubit pair $i < j$, the covariances (18) are to be measured for each initial state of the spectator qubits in the correlation neighborhood \mathcal{B}_{ij} , of which there are $2^{|\mathcal{B}_{ij}|}$. Let

$$k = \max_{ij} \{|\mathcal{A}_i|, |\mathcal{B}_{ij}|\} \quad (27)$$

be the number of qubits in the largest correlation neighborhood. Then a total of $O(2^k n^2)$ characterization measurements are required by our protocol.

IV. APPLICATION TO TRANSMON QUBITS

In this section we demonstrate and validate the technique using the IBM Q online device `ibmq_16_melbourne`, on registers of up to 9 superconducting transmon qubits. The chip layout is shown in Fig. 1. Each circuit was measured with 32k measurement samples.

To achieve high accuracy we choose $\epsilon_A = \epsilon_B = 10^{-3}$. We find that, for this tolerance, *all* of the qubits in the device are in the correlation volume. This is evident in Fig. 2, which shows the measured A_{ij} correlators for $n = 7$. Some of the A_{ij} are large and long-ranged. For example, $|A_{2,5}| > 1\%$, even though qubits Q_2 and Q_5 are separated from each other (see Fig. 1). The `ibmq_16_melbourne` crosstalk is therefore large on the scale of accuracy we are targeting. This means that the filtering step discussed in Sec. III C did not lower our required circuit count. Only when a register is *larger* than the correlation volume do we benefit from scalability.

We begin with the $n = 4$ register $\{Q_0, Q_1, Q_2, Q_3\}$, which is small enough to allow us to examine explicit T matrices. First we assume uncorrelated SPAM errors. The T matrix in the product approximation (2) is

$$T_{\text{prod}} = \begin{pmatrix} 0.9357 & 0.0546 & 0.0975 & 0.0058 & 0.0760 & 0.0054 & 0.0076 & 0.0005 & 0.0528 & 0.0032 & 0.0071 & 0.0004 & 0.0045 & 0.0003 & 0.0004 & 0 \\ 0.0330 & 0.9148 & 0.0034 & 0.0938 & 0.0026 & 0.0763 & 0.0003 & 0.0070 & 0.0019 & 0.0518 & 0.0003 & 0.0072 & 0.0002 & 0.0043 & 0 & 0.0004 \\ 0.0008 & 0.0001 & 0.8264 & 0.0500 & 0.0001 & 0 & 0.0726 & 0.0050 & 0.0001 & 0 & 0.0530 & 0.0034 & 0 & 0 & 0.0042 & 0.0003 \\ 0 & 0.0010 & 0.0291 & 0.8094 & 0 & 0.0001 & 0.0026 & 0.0670 & 0 & 0 & 0.0019 & 0.0544 & 0 & 0 & 0.0002 & 0.0037 \\ 0.0242 & 0.0014 & 0.0040 & 0.0002 & 0.8852 & 0.0609 & 0.0834 & 0.0060 & 0.0014 & 0.0001 & 0.0004 & 0 & 0.0500 & 0.0036 & 0.0050 & 0.0004 \\ 0.0009 & 0.0237 & 0.0001 & 0.0035 & 0.0309 & 0.8523 & 0.0030 & 0.0804 & 0.0001 & 0.0013 & 0 & 0.0004 & 0.0017 & 0.0499 & 0.0002 & 0.0047 \\ 0 & 0 & 0.0339 & 0.0019 & 0.0010 & 0 & 0.7980 & 0.0581 & 0 & 0 & 0.0033 & 0.0002 & 0 & 0 & 0.0480 & 0.0035 \\ 0 & 0 & 0.0012 & 0.0305 & 0 & 0.0006 & 0.0288 & 0.7722 & 0 & 0 & 0.0001 & 0.0033 & 0 & 0 & 0.0018 & 0.0439 \\ 0.0051 & 0.0002 & 0.0004 & 0 & 0.0003 & 0 & 0 & 0 & 0.8866 & 0.0530 & 0.1008 & 0.0060 & 0.0755 & 0.0050 & 0.0069 & 0.0005 \\ 0.0002 & 0.0041 & 0 & 0.0005 & 0 & 0.0003 & 0 & 0 & 0.0314 & 0.8676 & 0.0035 & 0.0963 & 0.0026 & 0.0691 & 0.0003 & 0.0066 \\ 0 & 0 & 0.0035 & 0.0002 & 0 & 0 & 0.0003 & 0 & 0.0011 & 0 & 0.7489 & 0.0454 & 0.0001 & 0 & 0.0656 & 0.0049 \\ 0 & 0 & 0.0001 & 0.0040 & 0 & 0 & 0.0003 & 0 & 0.0005 & 0.0263 & 0.7305 & 0 & 0 & 0 & 0.0025 & 0.0615 \\ 0.0001 & 0 & 0 & 0 & 0.0038 & 0.0003 & 0.0003 & 0 & 0.0237 & 0.0013 & 0.0062 & 0.0004 & 0.8357 & 0.0584 & 0.0791 & 0.0062 \\ 0 & 0.0001 & 0 & 0 & 0.0001 & 0.0038 & 0 & 0.0003 & 0.0008 & 0.0212 & 0.0002 & 0.0058 & 0.0291 & 0.8088 & 0.0030 & 0.0777 \\ 0 & 0 & 0.0001 & 0 & 0 & 0 & 0.0029 & 0.0002 & 0 & 0 & 0.0462 & 0.0027 & 0.0006 & 0 & 0.7544 & 0.0581 \\ 0 & 0 & 0 & 0.0001 & 0 & 0 & 0.0001 & 0.0029 & 0 & 0 & 0.0016 & 0.0437 & 0 & 0.0006 & 0.0284 & 0.7276 \end{pmatrix}$$

This should be compared to the exact (directly measured) T matrix, which is

$$T = \begin{pmatrix} 0.9368 & 0.0547 & 0.0880 & 0.0062 & 0.0764 & 0.0049 & 0.0087 & 0.0005 & 0.0530 & 0.0032 & 0.0053 & 0.0007 & 0.0052 & 0.0004 & 0.0005 & 0 \\ 0.0319 & 0.9147 & 0.0028 & 0.0836 & 0.0020 & 0.0768 & 0 & 0.0073 & 0.0014 & 0.0511 & 0.0002 & 0.0056 & 0.0001 & 0.0046 & 0 & 0.0003 \\ 0.0008 & 0.0001 & 0.8367 & 0.0498 & 0.0002 & 0 & 0.0729 & 0.0054 & 0.0001 & 0 & 0.0450 & 0.0031 & 0 & 0 & 0.0047 & 0.0004 \\ 0 & 0.0009 & 0.0290 & 0.8194 & 0 & 0.0001 & 0.0017 & 0.0662 & 0 & 0.0001 & 0.0012 & 0.0459 & 0 & 0 & 0.0001 & 0.0044 \\ 0.0232 & 0.0011 & 0.0138 & 0.0009 & 0.8847 & 0.0612 & 0.0827 & 0.0058 & 0.0017 & 0.0001 & 0.0114 & 0.0008 & 0.0496 & 0.0043 & 0.0059 & 0.0003 \\ 0.0018 & 0.0240 & 0.0006 & 0.0127 & 0.0315 & 0.8520 & 0.0027 & 0.0804 & 0 & 0.0019 & 0.0003 & 0.0109 & 0.0014 & 0.0488 & 0.0003 & 0.0046 \\ 0 & 0 & 0.0235 & 0.0011 & 0.0009 & 0.0001 & 0.7973 & 0.0581 & 0 & 0 & 0.0027 & 0.0001 & 0.0001 & 0 & 0.0472 & 0.0039 \\ 0 & 0 & 0.0014 & 0.0214 & 0 & 0.0004 & 0.0304 & 0.7726 & 0 & 0 & 0.0001 & 0.0023 & 0 & 0 & 0.0011 & 0.0430 \\ 0.0050 & 0.0004 & 0.0004 & 0 & 0.0003 & 0 & 0 & 0 & 0.8872 & 0.0533 & 0.0841 & 0.0049 & 0.0758 & 0.0055 & 0.0073 & 0.0006 \\ 0.0002 & 0.0039 & 0 & 0.0004 & 0 & 0.0003 & 0 & 0.0001 & 0.0310 & 0.8679 & 0.0026 & 0.0784 & 0.0017 & 0.0681 & 0.0002 & 0.0074 \\ 0 & 0 & 0.0035 & 0.0003 & 0 & 0 & 0.0002 & 0 & 0.0012 & 0.0002 & 0.7763 & 0.0468 & 0.0001 & 0 & 0.0653 & 0.0039 \\ 0 & 0 & 0.0002 & 0.0040 & 0 & 0 & 0 & 0.0003 & 0 & 0.0004 & 0.0272 & 0.7583 & 0 & 0.0001 & 0.0020 & 0.0609 \\ 0.0002 & 0 & 0 & 0 & 0.0038 & 0.0004 & 0.0005 & 0 & 0.0225 & 0.0008 & 0.0143 & 0.0011 & 0.8350 & 0.0571 & 0.0775 & 0.0060 \\ 0 & 0.0001 & 0 & 0 & 0.0001 & 0.0037 & 0 & 0.0003 & 0.0018 & 0.0212 & 0.0005 & 0.0142 & 0.0304 & 0.8106 & 0.0032 & 0.0773 \\ 0 & 0 & 0.0001 & 0 & 0 & 0 & 0.0029 & 0.0002 & 0 & 0 & 0.0270 & 0.0012 & 0.0006 & 0.0001 & 0.7552 & 0.0590 \\ 0 & 0 & 0 & 0.0002 & 0 & 0 & 0 & 0.0029 & 0 & 0 & 0.0019 & 0.0258 & 0 & 0.0005 & 0.0295 & 0.7281 \end{pmatrix}$$

While T_{prod} is similar to T , there are significant differences caused by correlated multiqubit measurement errors. We quantify these differences by two matrix norms, the Frobenius and max norm: $\|T_{\text{prod}} - T\|_{\text{fro}} = 0.0644$ and $\|T_{\text{prod}} - T\|_{\text{max}} = 0.0278$. In particular, the max norm indicates that neglecting SPAM correlation leads to $> 2\%$ errors in one or more individual matrix elements.

Next we include the leading-order SPAM error correlations. Including pair correlations leads to the approximate result $T_{\text{approx}} = T_{\text{prod}} + T_{\text{pair}}$ given by

$$T_{\text{approx}} = \begin{pmatrix} 0.9369 & 0.0547 & 0.0880 & 0.0062 & 0.0764 & 0.0049 & 0.0086 & 0.0005 & 0.0531 & 0.0032 & 0.0132 & 0.0009 & 0.0052 & 0.0004 & 0.0006 & 0 \\ 0.0319 & 0.9147 & 0.0028 & 0.0836 & 0.0021 & 0.0769 & 0.0001 & 0.0072 & 0.0013 & 0.0512 & 0.0004 & 0.0133 & 0.0001 & 0.0046 & 0 & 0.0005 \\ 0.0007 & 0.0001 & 0.8367 & 0.0498 & 0.0002 & 0 & 0.0731 & 0.0054 & 0.0001 & 0 & 0.0373 & 0.0028 & 0 & 0 & 0.0046 & 0.0003 \\ 0.0001 & 0.0009 & 0.0290 & 0.8194 & 0 & 0.0001 & 0.0015 & 0.0663 & 0 & 0.0001 & 0.0008 & 0.0382 & 0 & 0 & 0.0001 & 0.0043 \\ 0.0231 & 0.0011 & 0.0138 & 0.0008 & 0.8847 & 0.0612 & 0.0829 & 0.0057 & 0.0016 & 0.0001 & 0.0034 & 0.0002 & 0.0496 & 0.0042 & 0.0059 & 0.0004 \\ 0.0019 & 0.0240 & 0.0006 & 0.0127 & 0.0315 & 0.8519 & 0.0026 & 0.0805 & 0.0001 & 0.0019 & 0.0001 & 0.0034 & 0.0015 & 0.0488 & 0.0002 & 0.0043 \\ 0.0001 & 0 & 0.0235 & 0.0012 & 0.0009 & 0.0001 & 0.7971 & 0.0582 & 0 & 0 & 0.0105 & 0.0006 & 0.0001 & 0 & 0.0472 & 0.0038 \\ 0 & 0.0001 & 0.0015 & 0.0214 & 0 & 0.0005 & 0.0305 & 0.7725 & 0 & 0 & 0.0004 & 0.0098 & 0 & 0 & 0.0012 & 0.0432 \\ 0.0049 & 0.0004 & 0.0004 & 0 & 0.0004 & 0 & 0 & 0 & 0.8872 & 0.0533 & 0.0764 & 0.0049 & 0.0758 & 0.0055 & 0.0072 & 0.0005 \\ 0.0002 & 0.0039 & 0 & 0.0004 & 0 & 0.0002 & 0 & 0 & 0.0311 & 0.8678 & 0.0022 & 0.0703 & 0.0017 & 0.0681 & 0.0002 & 0.0074 \\ 0 & 0 & 0.0036 & 0.0002 & 0 & 0 & 0.0001 & 0 & 0.0012 & 0.0001 & 0.7838 & 0.0468 & 0.0001 & 0 & 0.0655 & 0.0041 \\ 0 & 0 & 0.0002 & 0.0041 & 0 & 0 & 0 & 0.0004 & 0 & 0.0004 & 0.0277 & 0.7663 & 0 & 0.0001 & 0.0019 & 0.0609 \\ 0.0002 & 0 & 0.0001 & 0 & 0.0038 & 0.0004 & 0.0004 & 0 & 0.0226 & 0.0007 & 0.0221 & 0.0014 & 0.8350 & 0.0571 & 0.0775 & 0.0060 \\ 0 & 0.0001 & 0 & 0.0001 & 0.0001 & 0.0037 & 0 & 0.0003 & 0.0017 & 0.0212 & 0.0008 & 0.0220 & 0.0304 & 0.8105 & 0.0033 & 0.0774 \\ 0 & 0 & 0 & 0 & 0 & 0 & 0.0030 & 0.0002 & 0 & 0 & 0.0194 & 0.0009 & 0.0006 & 0.0001 & 0.7552 & 0.0589 \\ 0 & 0 & 0 & 0.0001 & 0 & 0 & 0 & 0.0029 & 0 & 0 & 0.0014 & 0.0181 & 0 & 0.0005 & 0.0295 & 0.7280 \end{pmatrix}$$

Now the agreement with the directly measured T matrix is much better: $\|T_{\text{approx}} - T\|_{\text{fro}} = 0.0311$ and $\|T_{\text{approx}} - T\|_{\text{max}} = 0.0081$.

This performance persists for larger registers as well. In Table II we summarize the results of the same analysis for up to nine qubits. The $n = 9$ data implies that each of the more than quarter million independent matrix elements is estimated to better than 0.5% by the pair correlation method.

V. CONCLUSION

Motivated by a common SPAM error mitigation technique [3–11], we develop and apply an $O(n^2)$ method to characterize and correct correlated multiqubit SPAM errors on a register of n qubits. The technique assumes that correlated SPAM errors are dominated by pair correlations, and that, for large n , the range of the multiqubit measurement error correlations do not grow with system size.

There are a few natural extensions of the pair-correlation technique. One is to include the triple cor-

TABLE II. Accuracy of scalable T matrix estimation on ibmq_16_melbourne qubits $Q_0, Q_1, Q_2, \dots, Q_{n-1}$.

n	$\ T - I\ _{\text{fro}}$	$\ T_{\text{approx}} - T\ _{\text{fro}}$	$\ T_{\text{approx}} - T\ _{\text{max}}$
5	1.56	0.043	0.009
7	4.07	0.064	0.007
8	5.06	0.012	0.001
9	7.98	0.021	0.001

relations (17), which leads to an $O(n^3)$ method. Another is to employ the pair-correlation functions in a Gaussian error model. In this case the odd-order correlations will vanish and the even-order ones are determined by Isserlis's (or Wick's) theorem [14]. However, we did not find either extension to significantly improve the accuracy of the estimate for T .

The main weakness of our technique and the principle roadblock preventing application to even larger registers is the *classical* processing used in the evaluation of T_{pair} , which has complexity $O(n^3 4^n)$. We hope to address this limitation in the future.

ACKNOWLEDGMENTS

Data was taken using the BQP software package developed by the authors. We thank Robin Blume-Kohout, Ken Brown, Shantanu Debnath, Jay Gambetta, Sasha Korotkov, Matthew Neeley, and Erik Nielsen for their private communication. We're also grateful to IBM Research for making their devices available to the quantum computing community. This work does not reflect the views or opinions of IBM or any of their employees.

-
- [1] D. A. Lidar and T. A. Braun, *Quantum Error Correction* (Cambridge, 2013).
- [2] A. G. Fowler, M. Mariantoni, J. M. Martinis, and A. N. Cleland, Phys. Rev. A **86**, 032324 (2012).
- [3] R. C. Bialczak, M. Ansmann, M. Hofheinz, E. Lucero, M. Neeley, A. D. O'Connell, D. Sank, H. Wang, J. Wenner, M. Steffen, A. N. Cleland, and J. M. Martinis, Nature Physics **6**, 409 (2010).
- [4] M. Neeley, R. C. Bialczak, M. Lenander, E. Lucero, M. Mariantoni, A. D. O'Connell, D. Sank, H. Wang, M. Weides, J. Wenner, Y. Yin, T. Yamamoto, A. N. Cleland, and J. M. Martinis, Nature **467**, 570 (2010).
- [5] E. Magesan, J. M. Gambetta, A. D. Córcoles, and J. M. Chow, Phys. Rev. Lett. **114**, 200501 (2015).
- [6] S. Debnath, N. M. Linke, C. Figgatt, K. A. Landsman, K. Wright, and C. Monroe, Nature **536**, 63 (2016).
- [7] C. Song, K. Xu, W. Liu, C.-p. Yang, S.-B. Zheng, H. Deng, Q. Xie, K. Huang, Q. Guo, L. Zhang, P. Zhang, D. Xu, D. Zheng, X. Zhu, H. Wang, Y.-A. Chen, C.-Y. Lu, S. Han, and J.-W. Pan, Phys. Rev. Lett. **119**, 180511 (2017).
- [8] V. Havlicek, A. D. Corcoles, K. Temme, A. W. Harrow, J. M. Chow, and J. M. Gambetta, arXiv:1804.11326 (2018).
- [9] M. Gong, M.-C. Chen, Y. Zheng, S. Wang, C. Zha, H. Deng, Z. Yan, H. Rong, Y. Wu, S. Li, F. Chen, Y. Zhao, F. Liang, J. Lin, Y. Xu, C. Guo, L. Sun, A. D. Castellano, H. Wang, C. Peng, C.-Y. Lu, X. Zhu, and J.-W. Pan, Phys. Rev. Lett. **122**, 1 (2019), arXiv:1811.02292.
- [10] X. Wei, K., I. Lauer, S. Srinivasan, N. Sundaresan, D. T. McClure, D. Toyli, D. C. McKay, J. M. Gambetta, and S. Sheldon, arXiv: 1905.05720 (2019).
- [11] M.-C. Chen, M. Gong, X.-S. Xu, X. Yuan, J.-W. Wang, C. Wang, C. Ying, J. Lin, Y. Xu, Y. Wu, S. Wang, H. Deng, F. Liang, C.-Z. Peng, S. C. Benjamin, X. Zhu, C.-Y. Lu, and J.-W. Pan, arXiv: 1905.03150 (2019).
- [12] We avoid this issue by minimizing $\|T p_{\text{corr}} - p_{\text{raw}}\|_2^2$ subject to physicality constraints $0 \leq p_{\text{corr}}(x) \leq 1$ and $\|p_{\text{corr}}\|_1 = 1$.
- [13] The associated noninteracting system does not itself have to be experimentally realizable. For example, trapped ions can be spatially separated to turn off their qubit-qubit interaction, so in this case the noninteracting system is in principle realizable (by separating the qubits). However in solid-state architectures such as superconducting qubits, some stray qubit-qubit and detector-detector couplings are always present.
- [14] L. Isserlis, Biometrika **12**, 134 (1918).